

# Insights into How RNase R Degrades Structured RNA: Analysis of the Nuclease Domain

Helen A. Vincent and Murray P. Deutscher\*

Department of Biochemistry and Molecular Biology, University of Miami Miller School of Medicine, Miami, FL 33101, USA

Received 24 November 2008;  
received in revised form  
29 January 2009;  
accepted 31 January 2009  
Available online  
10 February 2009

RNase R readily degrades highly structured RNA, whereas its paralogue, RNase II, is unable to do so. Furthermore, the nuclease domain of RNase R, devoid of all canonical RNA-binding domains, is sufficient for this activity. RNase R also binds RNA more tightly within its catalytic channel than does RNase II, which is thought to be important for its unique catalytic properties. To investigate this idea further, certain residues within the nuclease domain channel of RNase R were changed to those found in RNase II. Among the many examined, we identified one amino acid residue, R572, that has a significant role in the properties of RNase R. Conversion of this residue to lysine, as found in RNase II, results in weaker substrate binding within the nuclease domain channel, longer limit products, increased activity against a variety of substrates and a faster substrate on-rate. Most importantly, the mutant encounters difficulty in degrading structured RNA, pausing within a double-stranded region. Additional studies show that degradation of structured substrates is dependent upon temperature, suggesting a role for thermal breathing in the mechanism of action of RNase R. On the basis of these data, we propose a model in which tight binding within the nuclease domain allows RNase R to capitalize on the natural thermal breathing of an RNA duplex to degrade structured RNAs.

© 2009 Elsevier Ltd. All rights reserved.

Edited by D. E. Draper

**Keywords:** RNase R; RNase II; RNA degradation; RNA binding; *Escherichia coli* ribonuclease

## Introduction

RNA degradation is an essential component of RNA metabolism. Ribonucleases (RNases) are required for the maturation of stable RNAs and for the removal of defective or redundant RNA species from the cell. In *Escherichia coli*, mRNA decay is carried out primarily by RNase II and polynucleotide phosphorylase (PNPase),<sup>1</sup> although structured mRNAs can be degraded only by PNPase<sup>2</sup> or a third enzyme, RNase R.<sup>2,3</sup> Similarly, PNPase and/or RNase R are required for the degradation of the highly structured rRNA<sup>4</sup> and tRNA<sup>5</sup> molecules (S.

Chebolu, C. Kim, E. Quesada and M. P. Deutscher, personal communication).

RNase R and RNase II belong to the RNR family of processive, hydrolytic 3' to 5' exoribonucleases. Nevertheless, consistent with their respective functions *in vivo*, their catalytic properties differ significantly.<sup>6,7</sup> RNase II is specific for single-stranded RNA, generally stalling 6–11 nucleotides before a duplex.<sup>3,8–10</sup> In contrast, RNase R is able to degrade through an RNA duplex, provided there is a 3' single-stranded overhang to which it can bind and initiate degradation.<sup>3,11</sup> RNase R is the only 3' to 5' exoribonuclease able to degrade through extensive secondary structure without the aid of helicase activity. Consequently, its mode of action is of great interest.

Relatively unstructured substrates such as poly(A) are degraded by both RNase R and RNase II, but differences are discernible even with these substrates. Single-stranded RNA is degraded by RNase II at least fourfold faster than by RNase R.<sup>12</sup> Moreover, RNase II becomes distributive as the substrate is degraded to pieces shorter than 10

\*Corresponding author. E-mail address: mdeutsch@med.miami.edu.

Present address: H. A. Vincent, University of Portsmouth, School of Biological Sciences, Portsmouth, PO1 2DY, UK.

Abbreviations used: RNase, ribonuclease; CSD, cold-shock domain; PNPase, polynucleotide phosphorylase.

nucleotides,<sup>12,13</sup> typically releasing limit products of tetra- and pentanucleotides,<sup>3,12</sup> whereas RNase R remains processive and leaves di- and trinucleotides as the limits of digestion.<sup>3,12</sup>

RNase R and RNase II share a common domain organization, with two cold-shock domains (CSDs) near the N-terminus, a central nuclease domain, and an S1 domain near the C-terminus. Crystal structures of *E. coli* RNase II show that the CSDs and the S1 domain come together to form an RNA-binding clamp through which the substrate presumably passes en route to the catalytic center located at the base of a narrow channel within the nuclease domain.<sup>14,15</sup>

We have recently presented evidence that, while the CSDs and the S1 domain of RNase R appear to have a role in substrate binding and in ensuring efficient catalysis, especially for longer substrates, they are not essential for RNase R to degrade through double-stranded RNA.<sup>16</sup> Hence, the nuclease domain alone is sufficient to perform this function.<sup>16</sup> Furthermore, we found that the nuclease domain of RNase R binds RNA more tightly than the nuclease domain of RNase II.<sup>16</sup> This tighter binding may help to explain many of the differences between the catalytic properties of RNase R and RNase II; for example, the slower rate of degradation of single-stranded RNA and the greater processivity of RNase R relative to RNase II. It remains to be determined if tighter substrate binding within the catalytic channel can account for the ability of RNase R to degrade through duplex RNA.

On the basis of sequence alignments and the structural information available for RNR family proteins, we now identify residues within the nuclease domain of RNase R that contribute to tight substrate binding and the related RNase R-specific catalytic properties. We focus on residues that differ between RNase R and RNase II. Candidate residues in RNase R are mutated to the amino acid present in RNase II and the resulting mutant proteins are evaluated for their ability to digest double-stranded RNA. We examine in detail the mutant protein RNase R R572K, which releases longer limit products than wild-type RNase R, and binds A<sub>4</sub> with a higher dissociation constant ( $K_d$ ) value, indicating that this residue contributes to substrate binding within the nuclease domain channel. Furthermore, this mutant protein is more active, more distributive as substrates get shorter, and stalls more frequently than wild-type RNase R when encountering double-stranded RNA, all properties consistent with RNase II. We discuss the role that RNA binding may have in the degradation of structured RNA by RNase R, and show that the ability of RNase R to degrade through structured RNA is strongly dependent on temperature, suggesting that thermal breathing of the RNA may have an important role in the mechanism. From this and other available information, we propose a model to explain the ability of RNase R to degrade structured RNAs.

## Results

### Identification of residues within the nuclease domain channel of RNase R that determine the catalytic properties of RNase R

The nuclease domain of RNase R is sufficient for RNase R to degrade through double-stranded RNA.<sup>16</sup> Based upon the crystal structures of the homologous *E. coli* RNase II,<sup>14,15</sup> and *Saccharomyces cerevisiae* Rrp44 proteins,<sup>17</sup> this domain contains a narrow channel that can accommodate five single-stranded nucleotides. The catalytic center lies at the base of this channel.<sup>14,15,17</sup> It seemed most likely that the residues responsible for the ability of RNase R to degrade through duplex RNA would be those in the nuclease domain that interacted with the RNA substrate. Such residues could be located within the nuclease domain channel itself, where they could contribute directly to tighter RNA binding, or they could be at the entrance to the channel, where they could be actively involved in separation of the RNA strands.

For the purpose of this study, we defined the residues of the nuclease domain channel as all of those from the nuclease domain that lie within 5 Å of the RNA substrate. We then identified such residues in RNase II from the crystal structure of a catalytic site mutant in complex with single-stranded RNA<sup>14</sup> using PyMOL†. The equivalent residues were then identified in RNase R based upon sequence alignment of the two proteins using Clustal X.<sup>18</sup> Of the 45 residues that met this criterion, 21 were unchanged in RNase R compared to RNase II. The majority of these invariant residues corresponded to those that contact the single-stranded RNA in the RNase II crystal structure,<sup>14</sup> suggesting that similar contacts are made to the RNA by RNase R. Since the nuclease domain of RNase R is able to degrade structured RNA, while that from RNase II stalls at a duplex,<sup>16</sup> we reasoned that it was likely to be one or more of the variant amino acids that was responsible for the ability of RNase R to digest through structured RNA. Thus, we decided to focus on these 24 variant residues. Figure 1 illustrates the distribution of these residues throughout the nuclease domain channel.

### Construction of RNase R nuclease domain channel mutants

A series of mutant proteins was constructed to investigate the contribution that the variant residues of the RNase R nuclease domain channel make to substrate binding and exoribonuclease activity, particularly the ability to degrade through double-stranded RNA. In each of these mutants, one or more variant residues in the nuclease domain channel of RNase R was replaced by the equivalent amino acid(s) found in

† <http://www.pymol.org>

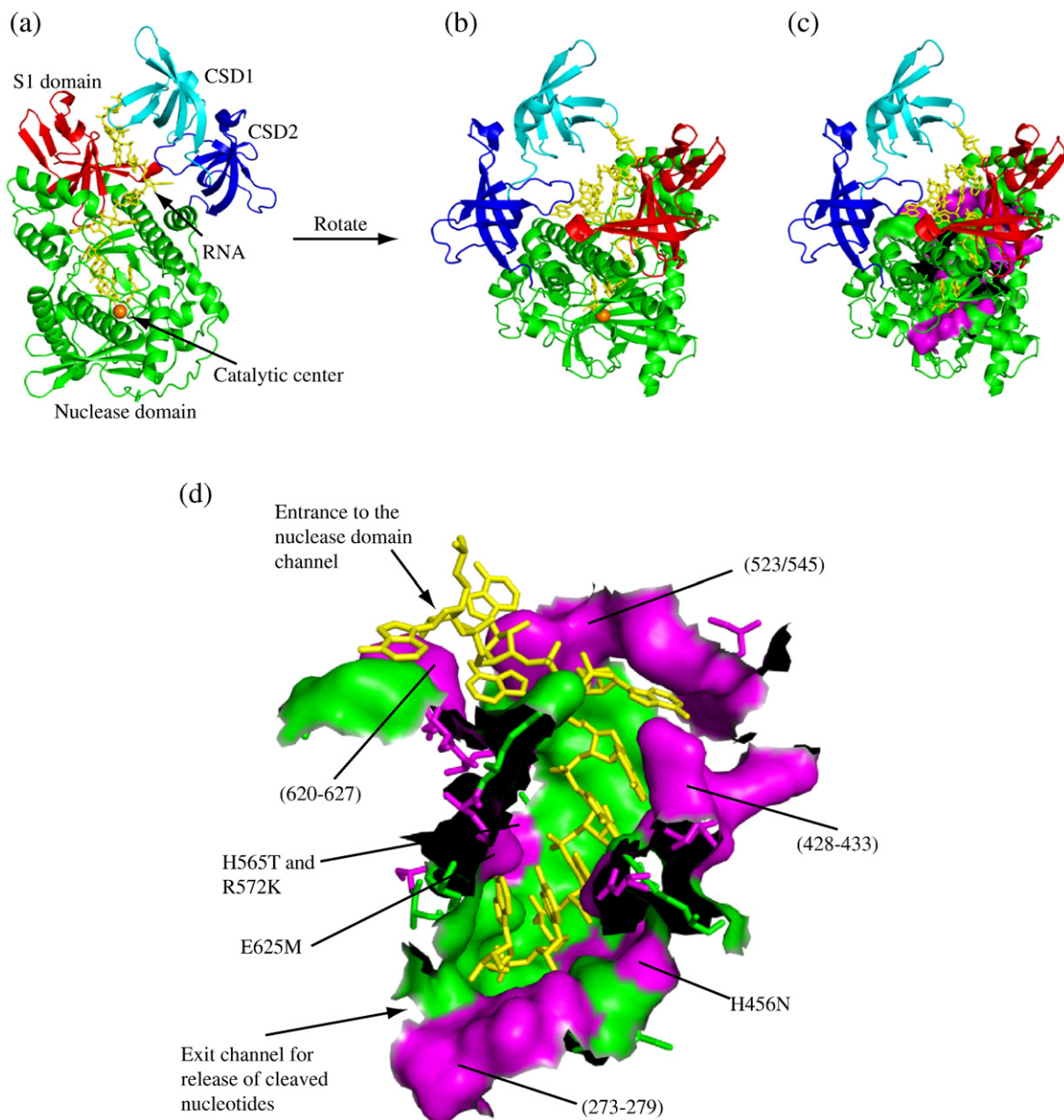


**Fig. 1.** Distribution of variant residues in the nuclease domain channel of RNase R. All panels were generated with PyMOL (<http://www.pymol.org>) based on the crystal structure of RNase II (PDB code 2IX1).<sup>14</sup> (a) A cartoon representation of RNase R clearly showing the path that the RNA takes between the cold-shock and S1 domains into the nuclease domain. The cold-shock domains are colored in cyan and blue for CSD1 and CSD2, respectively, the nuclease domain is green with the catalytic magnesium ion represented by an orange sphere and the S1 domain is red. The RNA substrate is shown as yellow sticks. (b) An alternative perspective of RNase R obtained by rotation of a; coloring is the same as in a. (c) The same as b with residues comprising the nuclease domain channel wall shown in a surface representation. Residues that are conserved between RNase R and RNase II remain in green and residues that differ are in magenta. (d) An enlarged surface representation of residues that form the nuclease domain channel wall. As in c, residues that are conserved between RNase R and RNase II are shown in green and residues that differ are in magenta. (The black areas are where amino acids have been removed to allow visualization of the channel). The approximate positions of the RNase R mutants constructed in this study are indicated. For orientation purposes, the entrance and exit of the channel are labeled.

RNase II. Using this approach, 23 of the 24 variant residues in the nuclease domain channel of RNase R were mutated. To simplify construction of the mutants, some residues that are not considered to be part of the nuclease domain channel, as defined above, were mutated in certain cases. A summary of the mutants, detailing which amino acids were changed in

each case, is given in Table 1. Although the nuclease domain alone is sufficient for RNase R activity, the level of activity observed with a truncated protein containing this domain alone is extremely low when compared to that of the full-length protein.<sup>16</sup> Consequently, the channel mutations were made in the context of full-length RNase R.

**Table 1.** RNase R nuclease domain channel mutants

RNase R mutant	Mutated residues	Location of the mutation in the nuclease domain channel
(273-279)	G273S, E274A, D275S, A276T, R277E, F279M	Base of the nuclease domain channel, near the catalytic center (by the phosphodiester bond between nucleotides 1 and 2) and the exit channel
(428-433)	S428F, F429K, E430D, S431R, E432P, E433D	Entrance to the nuclease domain channel, near the base moieties of nucleotides 5 and 6
H456N	H456N	Within the nuclease domain channel, nearest the base moiety of nucleotide 3
(523/545)	L523R, Q536D, L540R, M543Q, K544S, Q545F	Entrance to the nuclease domain channel, near nucleotides 6 and 7
H565T	H565T	Within the nuclease domain channel, near the phosphodiester bond between nucleotides 3 and 4
R572K	R572K	Within the nuclease domain channel, near the phosphodiester bonds between nucleotides 2 and 3, and nucleotides 3 and 4
(620-627)	E620R, R622L, A623N, D624R, E625M, T627E	Entrance to the nuclease domain channel, near nucleotides 5 – 7. E625 also appears to contact the base moiety of nucleotide 1

The residue numbers for the mutated residues correspond to the amino acid position in RNase R. Mutations in italics are residues that are not considered part of the nuclease domain channel based on the criteria discussed in Results. Nucleotide positions are numbered from the 3' end of the RNA chain.

### Screening of RNase R nuclease domain channel mutants

Wild-type RNase R, wild-type RNase II and each of the RNase R nuclease domain channel mutants listed in Table 1 were expressed in an *E. coli* strain lacking both RNase R and RNase II. Extracts containing the expressed proteins were prepared as described in Materials and Methods, and screened for activity using an electrophoretic assay with a substrate consisting of a (5'-<sup>32</sup>P)-labeled 34-mer annealed to a complementary 17-mer so as to generate a 17 bp duplex with a 17-nucleotide poly(A) 3' overhang (ds17-A<sub>17</sub>).

An extract expressing wild-type RNase R completely degraded the ds17-A<sub>17</sub> substrate (Fig. 2). However, in contrast to purified RNase R, which degrades this substrate to limit products of di- and trinucleotides,<sup>3,12</sup> some exoribonuclease activity in the wild-type extract led to further degradation, such that the labeled 5' residue was released as a mononucleotide. Most likely, RNase R degrades to the usual di- and trinucleotides, but oligoribonuclease, present in the extract, extends the degradation to mononucleotides. It should be noted that bands not typically observed in activity assays carried out with purified RNase R (see arrowheads in Fig. 2) are observed when using extracts, and presumably originate from the activity of enzymes other than RNase R. This could account for the low level of degradation that occurs with an extract that is not induced with IPTG and therefore does not express either RNase R or RNase II (see Fig. 2).

Similar to what is seen with purified RNase II, an extract from cells expressing RNase II is unable to degrade through the double-stranded region of ds17-A<sub>17</sub>, and stalls 7 – 9 nucleotides before the duplex region of this substrate (Fig. 2). This observation implies that any RNase R mutant that is significantly impaired in its ability to degrade double-stranded RNA, such that it behaves like RNase II, should be detectable within the context of an extract, allowing screening of the mutant proteins without having to purify each one.

However, as shown in Fig. 2, each of the extracts expressing an RNase R mutant protein was still able to degrade through the double-stranded region of ds17-A<sub>17</sub>, indicating that none of the variant nuclease domain channel residues, by itself, is responsible for the ability of RNase R to degrade structured RNAs. We did note that several mutant extracts (H565T, R572K and (620-627)) generated longer limit products compared to the wild-type extract, suggesting that the nuclease domains of these RNase R mutant proteins may bind to RNA more weakly. In fact, RNase II, which also releases longer limit products than RNase R, binds a tetranucleotide RNA molecule less tightly within its nuclease domain, as determined by a filter-binding assay.<sup>16</sup>

In the crystal structure of RNase II, the carboxyl group of E542 appears to be positioned to interact with the 3'-terminal nucleotide, where it can disrupt base-stacking, and assist in elimination of the cleaved nucleotide.<sup>14</sup> Disruption of this interaction would be expected to weaken substrate binding at the base of the nuclease domain channel. The sequence surrounding this amino acid is poorly conserved throughout the RNR family, and we initially identified the corresponding residue in RNase R as T627. However, it is more likely, given its proposed function, that this residue would be conserved between RNase II and RNase R, and that the corresponding residue in RNase R is actually E625. In the RNase R (620-627) mutant, E625 is changed to methionine, and it is possible that it is the mutation of a conserved amino acid that leads to the disruption of a conserved binding interaction and the longer limit products observed with the (620-627) mutant extract. Substitutions of amino acids typically conserved between RNase R and RNase II have been shown to affect the length of the limit products generated by RNase II.<sup>19</sup> Since E625 does not appear to account for the differences between RNase R and RNase II, the (620-627) mutant was not examined further.

In an attempt to obtain additional information on nuclease domain residues that might be important for RNase R activity on double-stranded RNA, the two other mutations that lead to the release of longer limit products, H565T and R572K, were combined to generate an RNase R H565T R572K double-mutant. A triple-mutant was constructed that combined the H565T and R572K mutations with H456N. Although an extract with H456N had similar activity to the wild-type extract (Fig. 2), the position of H456 in the nuclease domain channel suggested that further examination was warranted. H456 is near the base

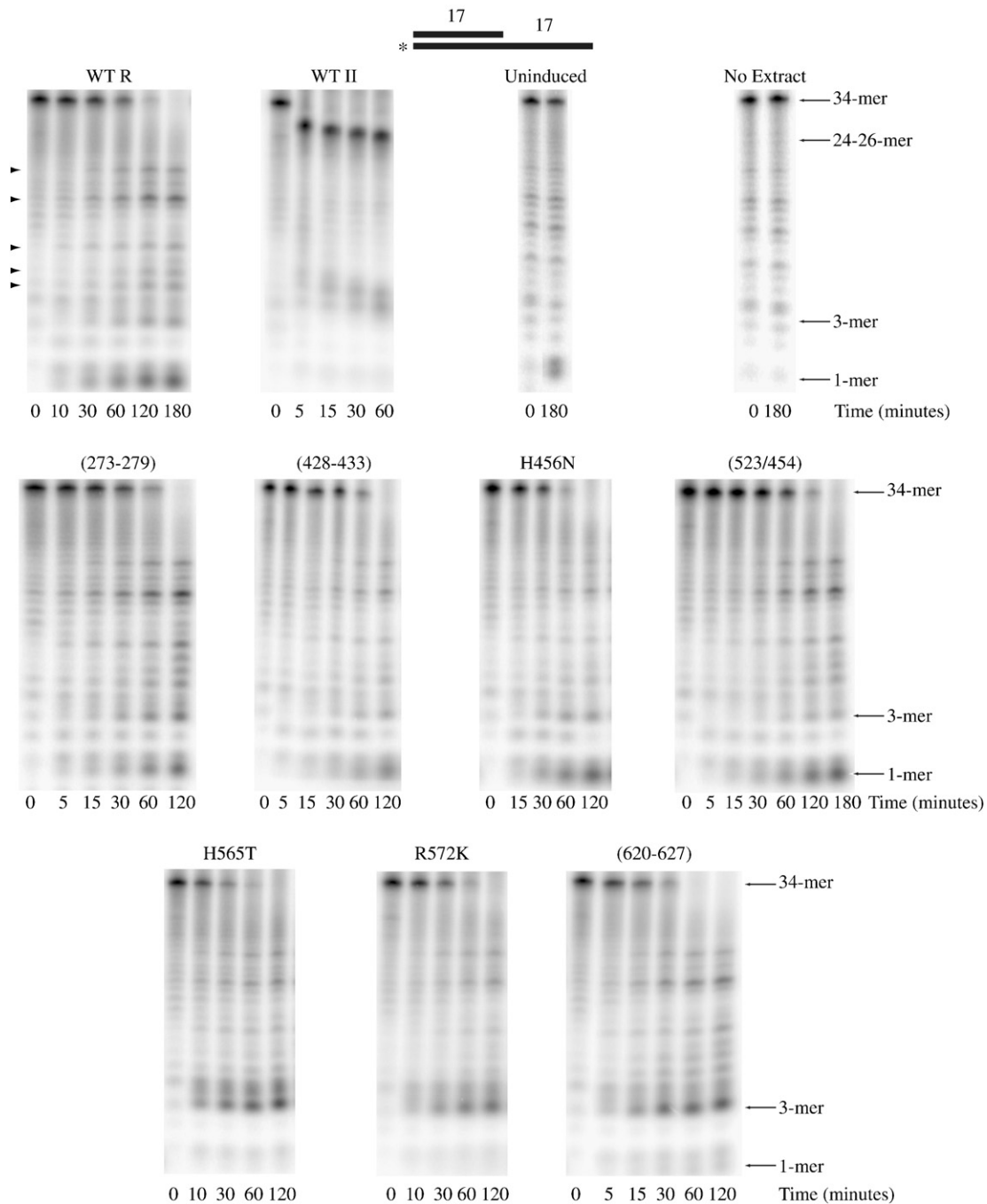


**Fig. 2.** Activity of nuclease domain channel mutant extracts on structured RNA. Assays were carried out as described in [Materials and Methods](#) with 10  $\mu$ M ds17-A<sub>17</sub> substrate and 2.5  $\mu$ g of wild-type RNase R, 0.5  $\mu$ g of wild-type RNase II, 2.5  $\mu$ g of uninduced, 2.5  $\mu$ g of RNase R (273-279), 2.5  $\mu$ g of RNase R (428-433), 5  $\mu$ g of RNase R H456N, 2.5  $\mu$ g of RNase R (523/545), 10  $\mu$ g of RNase R H565T, 2.5  $\mu$ g of RNase R R572K and 2.5  $\mu$ g of RNase R (620-627) cell extract. Aliquots were taken at the indicated times and analyzed by denaturing PAGE. A representation of the substrate is shown at the top of the figure with the position of the <sup>32</sup>P label denoted by an asterisk. Non-specific product bands that do not appear to originate from RNase R activity are indicated on the left of the wild-type RNase R panel by arrowheads.

moiety of nucleotide 3, whereas H565 and R572 are near the phosphodiester bonds connecting either nucleotides 3 and 4 or connecting both nucleotides 2 and 3 and 4, respectively.

Cell extracts were prepared from strains expressing either the double or triple-mutant, and their activity on ds17-A<sub>17</sub> was compared to wild-type RNase R and to the single H565T and R572K mutants. As shown in

[Fig. 3](#), the double and triple mutant extracts also were able to degrade through the double-stranded region of the ds17-A<sub>17</sub> substrate. As was found with the single mutants, these extracts generated longer limit products compared to wild-type RNase R extracts. These data indicate that the effect of the single H565T or R572K mutations is not accentuated by the presence of additional mutations with similar

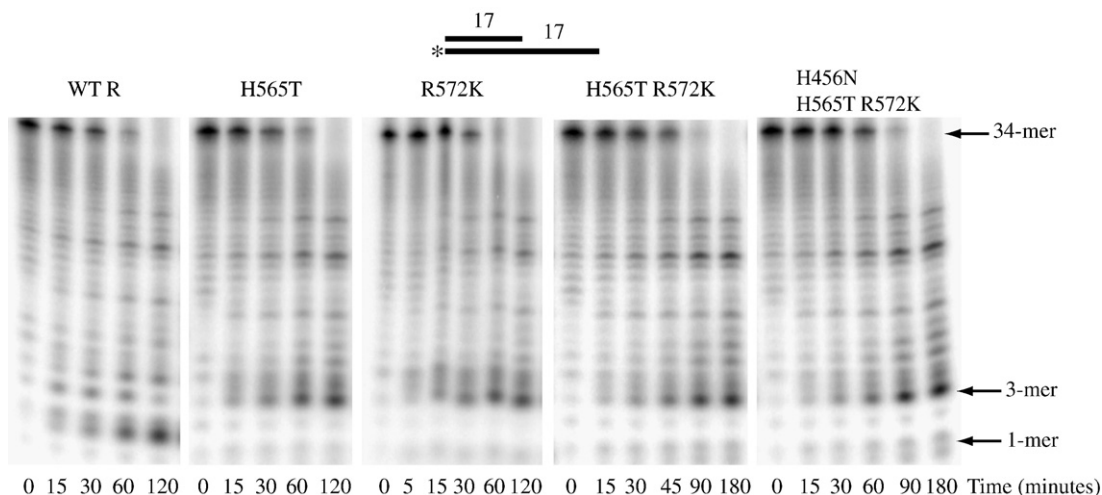


**Fig. 3.** Activity of RNase R H565T R572K and RNase R H456N H565T R572K on structured RNA. Assays were carried out as described in *Materials and Methods* with 10  $\mu$ M ds17-A<sub>17</sub> substrate and 2.5  $\mu$ g of wild-type RNase R, 10  $\mu$ g of H565T, 2.5  $\mu$ g of R572K, 2.5  $\mu$ g of H565T R572K and 5  $\mu$ g of H456N H565T R572K cell extract. Aliquots were taken at the indicated times and analyzed by denaturing PAGE. A representation of the substrate is shown at the top of the figure with the position of the <sup>32</sup>P label denoted by an asterisk.

properties. The most likely explanation for this is that mutating either of the neighboring H565 or R572 residues is sufficient to disrupt this region of the channel and eliminate protein–RNA contacts made by one or both of these amino acids.

**Characterization of purified RNase R R572K and RNase R H456N H565T R572K mutant proteins**

As discussed above, assays carried out with cell extracts generate a number of products that do not appear to originate from RNase R activity. Since these non-specific bands may mask subtle changes in the activity of the RNase R mutants relative to the wild-type enzyme, it seemed worthwhile to purify a single mutant, R572K, and the triple mutant, H456N H565T R572K, to characterize and compare their activities more carefully. The purity of these mutant proteins, as well as wild-type RNase R and RNase II, is shown in *Fig. 4*.

The activities of purified RNase R R572K and H456N H565T R572K were tested with ds17-A<sub>17</sub> and the corresponding single-stranded 34-mer, ss17-A<sub>17</sub>, as substrates. Wild-type RNase R and RNase II were used for comparison. As shown in *Fig. 5a*, all four proteins readily degrade the single-stranded 34-mer. As expected, wild-type RNase R released di- and trinucleotides as limit products, whereas RNase II released predominantly pentanucleotides as the limit of digestion. Confirming the data obtained with cell extracts, purified R572K and H456N H565T R572K released tri- and tetranucleotides. This is consistent with the RNase R mutants binding short oligoribonucleotides more weakly than wild-type RNase R, but more tightly than RNase II. We present evidence below that this is the case.

Degradation of ss17-A<sub>17</sub> by wild-type RNase R is highly processive, since only the original substrate and

the di- and trinucleotide limit products could be detected (*Fig. 5a*). This contrasts with RNase II, which becomes distributive as the substrate shortens; in addition to the tetra- and pentanucleotide limit products, bands can be detected that correspond to 7-, 9-, 10- and 13-mers. Interestingly, RNase R R572K also appears to stall, generating 7-, 13- and 17-mers.

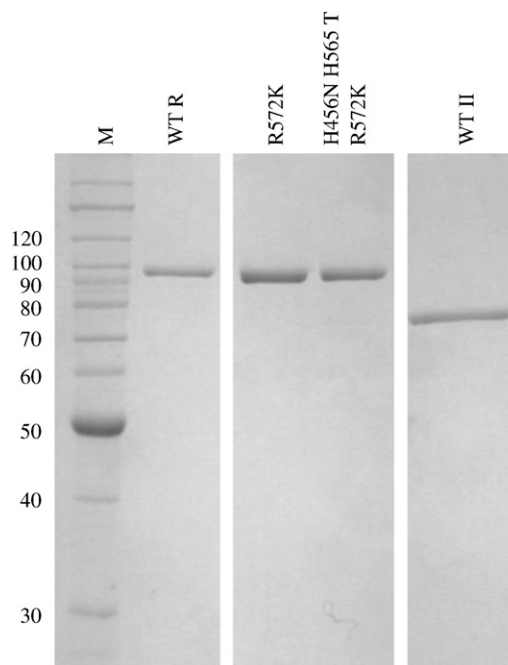


**Fig. 4.** Purity of RNase R mutants. A 1  $\mu$ g sample of purified wild-type RNase R, RNase R R572K, RNase R H456N H565T R572K and RNase II were resolved by SDS-PAGE (10% (w/v) acrylamide gel) and visualized by staining with Coomassie brilliant blue. The molecular masses (in kDa) of protein standards (M) are indicated on the left. Pure RNase II was obtained from Dr. A. Malhotra (University of Miami, Miami, FL).

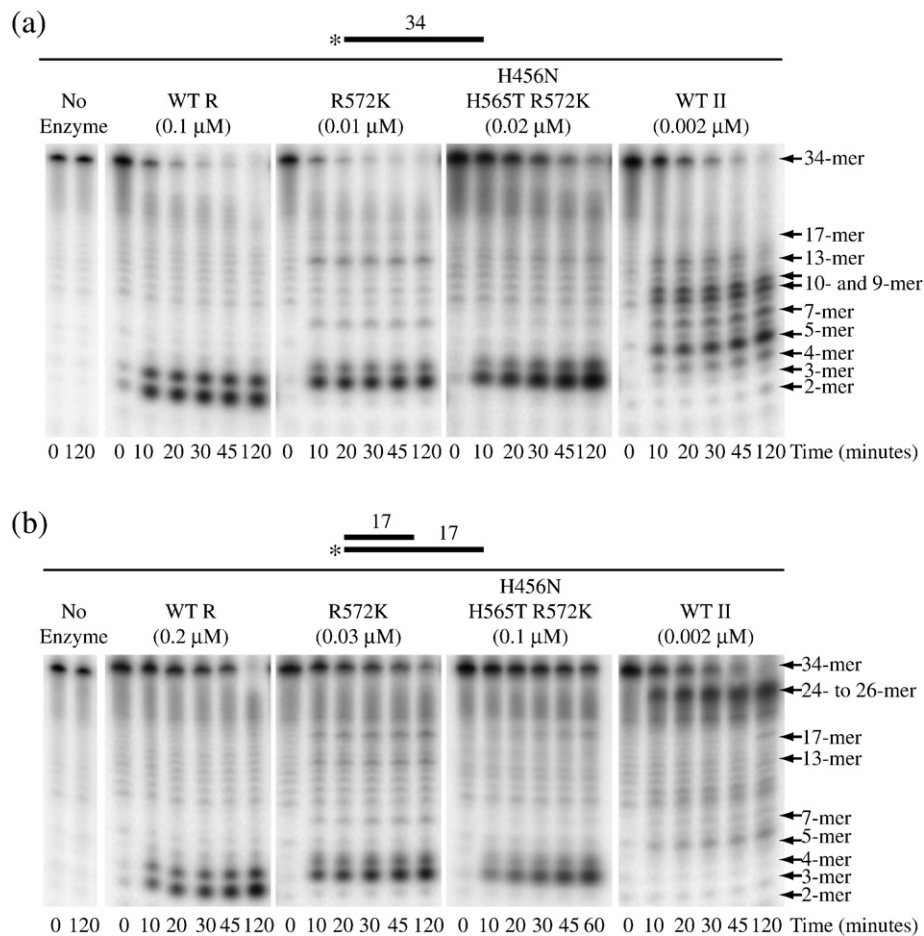


**Fig. 5.** Activity of purified RNase R R572K and RNase R H456N H565T R572K. Activity assays were done as described in [Materials and Methods](#). Aliquots were taken at the indicated times and analyzed by denaturing PAGE. (a) ss17-A<sub>17</sub> was present at 10 μM with 0.1 μM wild-type RNase R, 0.01 μM R572K, 0.02 μM H456N H565T R572K and 0.002 μM RNase II. (b) ds17-A<sub>17</sub> was present at 10 μM with 0.2 μM wild-type RNase R, 0.03 μM RNase R R572K, 0.1 μM RNase R H456N H565T R572K and 0.002 μM RNase II. A representation of the substrates is shown above each panel with the position of the <sup>32</sup>P label indicated by an asterisk.

Similar stalling was observed with the triple-mutant, but the effect appeared to be less pronounced. These data indicate that the R572K mutant behaves more like RNase II, and that this amino acid therefore has an important role in defining the catalytic properties of RNase R and RNase II.

To further investigate the activity of RNase R and RNase R R572K on ss17-A<sub>17</sub>, the enzymes were compared under single-turnover conditions. This was achieved by carrying out the assays at concentrations of substrate and enzyme above the determined  $K_d$  (see [Table 3](#) below) and with the enzyme present at fivefold excess over substrate.<sup>20</sup> Reactions were initiated by mixing RNase R with (5'-<sup>32</sup>P)-labeled ss17-A<sub>17</sub> substrate and quenching the reaction in the millisecond to second timescale using a rapid chemical-quench flow apparatus as described in [Materials and Methods](#). Reactions were analyzed by denaturing PAGE as described for the steady-state assays. Such experiments allow clearer visualization of reaction intermediates, as degradation of each substrate molecule is initiated at the same time. As shown in [Fig. 6](#), consistent with the steady-state

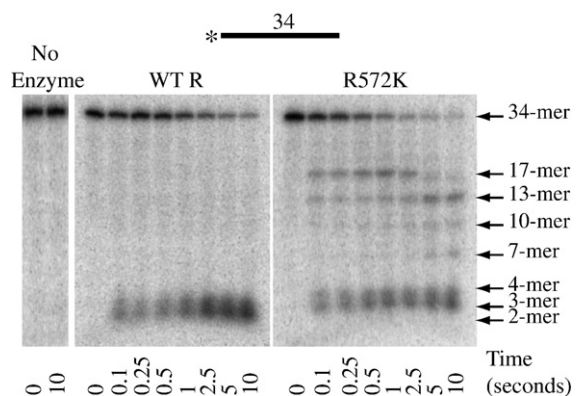


**Fig. 6.** Activity of purified wild-type RNase R and RNase R R572K under single-turnover conditions. Single-turnover experiments were carried out as described in [Materials and Methods](#). Reactions were allowed to proceed for the indicated lengths of time and analyzed by denaturing PAGE. A representation of the substrate is shown at the top of the figure with the position of the <sup>32</sup>P label indicated by an asterisk.

data, for wild-type RNase R, only the initial substrate or the limit products could be detected, even at the shortest time-point (0.1 s). This suggests that nucleotide cleavage is fast relative to binding and initiation of degradation. If we define the on-rate as including all possible mechanistic steps up to and including the cleavage of the first phosphodiester bond, this implies that the on-rate is rate-limiting for the reaction (see below). With R572K, again consistent with the steady-state data presented in Fig. 5a, multiple intermediate bands were detected that corresponded to 7-, 10-, 13- and 17-mers (Fig. 6). However, the substrate-product relationships are clearer in the single-turnover experiment, in that the 17-mer intermediate accumulates as the initial substrate disappears and the 13-mer is detected as the 17-mer disappears, and so on. Thus, these bands represent positions at which the enzyme pauses, rather than dissociates from the substrate. Moreover, based on the sequence of the substrate, these pauses occur as the enzyme encounters multiple pyrimidine residues.

On the ds17-A<sub>17</sub> substrate, under steady-state conditions, wild-type RNase R, R572K and H456N H565T R572K were able to degrade to completion, whereas RNase II stalled well before the duplex (Fig. 5b), as was found with cell extracts. Again, the limit products were tri- and tetranucleotides for the RNase R mutants compared to di- and trinucleotides for wild-type RNase R. The 7-, 13- and 17-mer products detected with the ss17-A<sub>17</sub> substrate were observed also with ds17-A<sub>17</sub>. However, the band at the position of the 17-mer was more pronounced when ds17-A<sub>17</sub> was used as the substrate (compare Fig. 5a and b). Since this position represents the single-strand/double-strand junction of the ds17-A<sub>17</sub> substrate, the data suggest that both R572K and H456N H565T R572K may have more difficulty in initiating degradation of the double-stranded region than does the wild-type protein.

The rates at which ss17-A<sub>17</sub> and ds17-A<sub>17</sub> were degraded by wild-type RNase R, R572K and H456N H565T R572K are shown in Table 2. The single- and triple-mutant proteins degrade both of these substrates at a considerably faster rate than wild-type RNase R. Although this may at first appear to contradict the data presented in Fig. 5, where the

mutants appear to degrade the substrates to the same extent as wild-type, the quantity of enzyme used in the assays shown was actually much lower than that used for wild-type RNase R. RNase II typically degrades unstructured substrates at a faster rate than RNase R,<sup>12</sup> suggesting that R572 is, at the least, an important determinant of the catalytic properties specific to RNase R.

ss17-A<sub>17</sub> is degraded ~15-fold faster by the single-mutant and ~5-fold faster by the triple-mutant, while ds17-A<sub>17</sub> is degraded ~10-fold and ~3-fold more rapidly by the single- and triple-mutant, respectively. Thus, although the mutants are more active than wild-type on both substrates, the relative increase was smaller on the ds17-A<sub>17</sub> substrate. This suggests that the mutants have more difficulty than the wild-type in degrading double-stranded relative to single-stranded RNA.

In an attempt to understand the reason for the overall faster rates of degradation by the RNase R mutants, activity was measured also on a variety of substrates. These included A<sub>17</sub>, C<sub>17</sub>, U<sub>17</sub> and ss17, which is the 5' 17 nucleotides of the ss17-A<sub>17</sub> and ds17-A<sub>17</sub> substrates. As shown in Table 2, wild-type RNase R displayed activity within the same range for all four of these substrates, suggesting that it has little sequence specificity. It has been reported that RNase R can show some sequence specificity when degrading homopolymers in the order poly(A) > poly(U) > poly(C).<sup>12</sup> However, those assays were carried out at 100 mM KCl rather than the 300 mM KCl used here, which may be responsible for the difference. In fact, RNase II also displays sequence specificity that is lost at high concentrations of salt.<sup>13,21</sup> Both RNase R R572K and RNase R H456N H565T R572K degraded A<sub>17</sub> at a rate similar to that of wild-type RNase R (Table 2), whereas C<sub>17</sub>, U<sub>17</sub> and ss17 were degraded at rates between 2- and 25-fold higher by the mutant enzymes (Table 2). Thus, mutation of R572 within the active site channel of RNase R can increase reaction rates dramatically, but this is strongly dependent on the nucleotide composition of the substrate.

Moreover, the experiments carried out under single-turnover conditions indicated that there is a significant increase in the on-rate (defined as the rate including all mechanistic steps up to and including the cleavage of the first phosphodiester bond) for RNA-binding by RNase R R572K compared to the wild-type enzyme. By measuring the rate of disappearance of the substrate, the on-rates were found to be 0.38 ± 0.1 s<sup>-1</sup> for wild-type RNase R and 4.6 ± 0.3 s<sup>-1</sup> for RNase R R572K with the ss17-A<sub>17</sub> substrate at 15 °C. This large difference in on-rates may explain the faster degradation rates observed for the R572K mutant compared to the wild-type enzyme under steady-state conditions, which involve multiple binding/initiation events over the course of an assay.

The finding that the R572K and H456N H565T R572K mutants stall more frequently and produce longer limit products than the wild-type protein

**Table 2.** Comparison of the activities of wild-type RNase R, RNase R R572K and RNase R H456N H565T R572K

Substrate	Activity (nmol min <sup>-1</sup> nmol <sup>-1</sup> RNase R)		
	Wild-type RNase R	RNase R R572K	RNase R H456N H565T R572K
ss17-A <sub>17</sub>	5.3 ± 1.6	75 ± 24	27 ± 12
ds17-A <sub>17</sub>	0.5 ± 0.2	5.1 ± 2.1	1.5 ± 0.4
A <sub>17</sub>	40 ± 4.8	41 ± 7.0	33 ± 8.5
C <sub>17</sub>	22 ± 13	130 ± 32	82 ± 28
U <sub>17</sub>	42 ± 14	170 ± 65	87 ± 28
ss17	29 ± 13	700 ± 99	200 ± 29

Activity assays were performed as described in Materials and Methods. Each value represents the mean of at least three experiments.

**Table 3.** RNA Binding to RNase R R572K

Substrate	$K_d$ (nM)	
	Wild-type RNase R	RNase R R572K
A <sub>17</sub>	0.8±0.1	0.5±0.1
A <sub>4</sub>	1200±90	5800±1,500

$K_d$  was determined by a filter-binding assay as described in [Materials and Methods](#). Each value represents the mean of at least two experiments.

suggests that they may bind RNA more weakly. To test this directly, the  $K_d$  for binding of A<sub>17</sub> and A<sub>4</sub> was measured for wild-type RNase R and R572K. As shown in [Table 3](#), both proteins bound A<sub>17</sub> with a similar  $K_d$ . However, the  $K_d$  value for A<sub>4</sub>, which should be bound entirely within the nuclease domain channel, was ~5-fold higher for the R572K mutant. This result indicates that R572 does contribute to substrate binding within the channel. Therefore, the mutation of R572 to lysine brings the catalytic properties of RNase R closer to those of RNase II which binds to A<sub>17</sub> with a  $K_d$  ~7-fold greater than that of RNase R and is unable to bind to A<sub>4</sub> in a filter-binding assay.<sup>16</sup>

### Effect of temperature on the degradation of structured RNA

One possibility for how RNase R degrades through structured RNA is that it exploits the transient opening of the RNA duplex that occurs during thermal breathing. For many enzyme-catalyzed reactions the temperature coefficient, or  $Q_{10}$ , (the factor by which the rate of a reaction increases for every 10 deg. C rise in temperature) is approximately 2. However, for biological processes requiring large conformational changes, such as thermal breathing of the RNA substrate,  $Q_{10}$  is often greater than 2. Consequently, it is possible to determine whether other factors may contribute to the mechanism of a reaction by investigating the change in reaction rate with increasing temperature.

To determine whether thermal breathing might contribute to the ability of RNase R to degrade structured RNA, rates of degradation of ss17-A<sub>17</sub> and ds17-A<sub>17</sub> were measured at 17 °C, 27 °C, 37 °C and 47 °C. If thermal breathing were involved, it would be expected that the rate on a structured substrate would be affected more than the rate on a single-stranded substrate by increasing the temperature of the reaction. This was found to be the case. For the single-stranded ss17-A<sub>17</sub> substrate  $Q_{10}$  was determined to be 1.8, consistent with the increase in temperature leading to an increase in the rate of the reaction chemistry. In contrast,  $Q_{10}$  for the structured ds17-A<sub>17</sub> substrate was found to be 3.6. The importance of this step to the mechanism is even more apparent when we compare the ratio of the rate on the structured substrate to that on the single-stranded substrate, thereby eliminating  $Q_{10}$  effects on the reaction chemistry. As shown in [Fig. 7](#), this ratio increases dramatically with increasing tem-

perature from 0.02 at 17 °C to 0.15 at 47 °C, indicating that there is an additional step, specific to the structured RNA, that contributes to the overall reaction. This step alone also has a  $Q_{10}$  of ~2.

Overall, these data are most consistent with a temperature-dependent conformational change, most likely thermal breathing of the RNA duplex, having an important role in the degradation of double-stranded RNA by RNase R.

## Discussion

Although both RNase R and RNase II belong to the RNR family of exoribonucleases,<sup>6,7</sup> there are significant differences in their catalytic properties. RNase II is limited to single-stranded regions,<sup>3,8-10</sup> while RNase R readily degrades through double-stranded RNA when provided with a single-stranded overhang to bind and initiate degradation.<sup>3,11</sup> We showed recently that the nuclease domain alone of RNase R is sufficient to perform this function.<sup>16</sup> Furthermore, RNase R binds RNA more tightly within its nuclease domain than RNase II.<sup>16</sup> This could explain the slower rates of degradation of single-stranded RNA relative to RNase II, and the maintenance of processivity even on very short oligoribonucleotides, resulting in the release of shorter limit products than RNase II.

The available crystal structures for RNase II provide an explanation for the single-strand specificity of this enzyme. In these structures, the path an RNA substrate must take between the CSDs and the S1 domain and into the nuclease domain is only wide enough to accommodate single-stranded

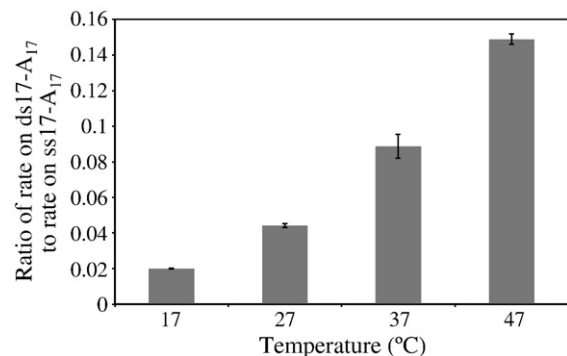


**Fig. 7.** Effect of temperature on the ability of RNase R to degrade structured RNA. Assays were carried out as described in [Materials and Methods](#), except they were performed at the indicated temperatures. ss17-A<sub>17</sub> was present at 10 μM with 0.07 μM wild-type RNase R or ds17-A<sub>17</sub> was present at 10 μM with 0.2 μM RNase R. Aliquots were taken during an appropriate time-course and analyzed by denaturing PAGE to measure linear degradation of the substrate. Results are plotted as a ratio of the rate on double-stranded RNA to the rate on single-stranded RNA. The values represent the mean of two experiments and the standard deviation is indicated (between two and four time-points were collected per experiment allowing determination of the standard deviation).

RNA.<sup>14,15</sup> Thus, although the RNA-binding domains constitute the initial barrier to double-stranded RNA,<sup>8,11,16</sup> the nuclease domain itself is unable to degrade duplex RNA.<sup>8,16</sup>

RNase R requires a 3' single-stranded overhang at least five nucleotides long in order to degrade through a double strand (our unpublished results).<sup>3,11,12</sup> Likewise, the yeast homologue of RNase R, Rrp44, requires a 3' overhang to degrade structured RNA.<sup>17,22</sup> On the basis of the crystal structure of this latter enzyme, its nuclease domain channel also is too narrow to allow entry of an RNA duplex.<sup>17</sup> This explains the requirement for a 3' single-stranded overhang on RNase R/Rrp44 substrates. Recent studies with Rrp44 have revealed that in addition to acting as an exoribonuclease it contains an endonuclease activity within its N-terminal PIN domain.<sup>23–25</sup> This activity may allow the generation of RNA fragments with the required single-stranded overhang for exoribonucleolytic degradation.<sup>23–25</sup> Furthermore, in contrast to RNase II, the nuclease domain alone of RNase R is able to degrade through double-stranded RNA,<sup>16</sup> suggesting that the nuclease domain of RNase R must unwind the duplex before its entrance into the channel in order to degrade the RNA.

In this study, we identified 24 residues within the nuclease domain channel of RNase R and RNase II that vary between the two enzymes and are, therefore, likely candidates for defining the catalytic properties of these enzymes and contributing to the ability of RNase R to degrade through double-stranded RNA. The majority of these variant residues were found around the entrance to the nuclease domain channel, where they could assist in duplex unwinding by intercalating between the bases of a double strand, a strategy employed by cold-shock proteins,<sup>26–28</sup> or form a structural wedge that separates the strands as the RNA is pulled across it during translocation, analogous to the "pin" region of RecBCD.<sup>29</sup> However, none of the proteins that were mutated in this region impaired the ability of RNase R to degrade through double-stranded RNA. Nevertheless, we cannot rule out the possibility that residues conserved between RNase R and RNase II adopt alternative conformations in the two proteins. In fact, three arginine residues that are conserved in RNase R, RNase II and Rrp44, are in a different position in the Rrp44 crystal structure compared with RNase II, such that they bind to the RNA substrate in Rrp44, but do not appear to do so in RNase II.<sup>17</sup>

We did identify at least one residue within the nuclease domain channel of RNase R that affected RNA binding and the ability of RNase R to initiate the degradation of structured substrates. Mutation of R572 or the neighboring H565 resulted in proteins that produced longer limit products, consistent with the fact that they bind to short oligoribonucleotides more weakly. Direct measurement of binding of A<sub>4</sub> to purified RNase R R572K confirmed that binding was weaker than that to the wild-type protein and, therefore, that the R572K mutation impairs substrate binding

within the nuclease domain channel. The purified R572K mutant also stalled more frequently than wild-type RNase R, including when approaching an RNA duplex. These data suggest that the ability to degrade through double-stranded RNA is related to the tight binding of the substrate in the nuclease domain channel of RNase R.

A mutational analysis of residues within the nuclease domain of RNase II found that a number of residues at the catalytic center of this enzyme affect both the length of the limit products produced and the affinity of the enzyme for RNA.<sup>19</sup> In this study, the amino acids that were mutated were those that are conserved between RNase R and RNase II.<sup>19</sup> Likewise, we found that mutation of the conserved E625 residue in RNase R led to the production of longer limit products.

The nuclease domain of RNase R binds considerably more tightly to RNA than the nuclease domain of RNase II,<sup>16</sup> and we believe that this property is important for RNase R to degrade structured RNA. As RNase R digests and moves into a double-stranded region, the very tight binding of single-stranded RNA within the channel may favor strand separation and translocation forward rather than dissociation of the substrate and reannealing of the opened base-pairs. This would be analogous to the role of single-stranded binding proteins in DNA recombination and repair.<sup>30</sup> Such a mechanism would allow RNase R to capitalize on the natural thermal breathing of the RNA duplex to move through the double-stranded region. The dramatic increase in activity on a structured substrate relative to single-stranded RNA as temperature is increased suggests that thermal breathing does have a role in the ability of RNase R to degrade structured RNA.

It is important to consider what happens to the displaced strand as RNase R degrades through a duplex. Binding and sequestration of this strand could assist in the unwinding process by preventing reannealing of the unwound bases. A region on the exterior of the nuclease domain may be able to perform this function. For example, it is possible that the alternate path between the nuclease domain and the CSDs that was proposed for RNase II,<sup>15</sup> and was observed in the Rrp44 crystal structure,<sup>17</sup> actually serves as an exit channel for the displaced strand of a duplex.

On the basis of the available data, we propose the following model to explain the ability of RNase R to degrade structured RNAs (Fig. 8a). RNase R initiates degradation of a structured substrate with a minimal 3' overhang of five nucleotides by binding the single-stranded region within its nuclease domain channel. Following cleavage and release of the 3' terminal nucleotide, translocation along the RNA substrate would be blocked by the RNA duplex. However, tight binding within the channel allows RNase R to remain bound at the single-strand/double-strand junction long enough to take advantage of thermal breathing events and thereby advance into the duplex. This process may be enhanced by residues at the entrance to the nuclease

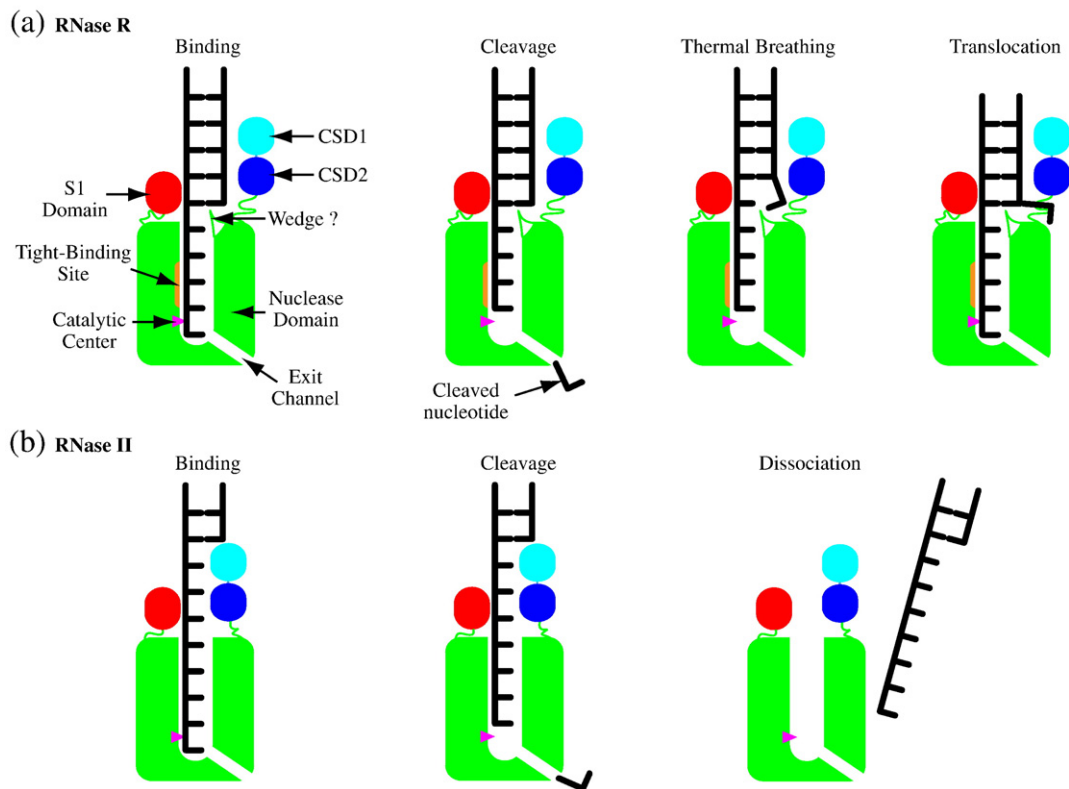


**Fig. 8.** A model for the mechanism of degradation of double-stranded RNA by RNase R. (a) RNase R; (b) RNase II. The RNA-binding domains are shown in cyan, blue and red for the CSD1s, CSD2s and S1 domains, respectively. The nuclease domains are in green with the catalytic centers shown as magenta triangles. In the binding step, RNase R or RNase II bind to the 3' single-stranded overhang of a structured RNA molecule. The 3'-terminal nucleotide is then cleaved and released. Translocation of both enzymes is blocked by the double-stranded region of the RNA. RNase R remains bound to the RNA substrate as the end of the duplex is opened by thermal breathing and/or a wedge at the entrance to the nuclease domain. RNase R translocates forward to position the RNA for the cleavage of the next nucleotide. In contrast, following nucleotide cleavage, the RNA dissociates from RNase II and prevents further degradation of the substrate.

domain channel that maintain the separation of the opened base-pairs. Translocation of RNase R along the RNA during this transient opening of the terminal base-pair of the duplex would be favored because it restores the binding interactions between the 3'-terminal nucleotide and the catalytic center that were lost by the previous cleavage event. In contrast, RNase II (Fig. 8b), which binds RNA more weakly within its channel, would dissociate from the RNA too rapidly to allow such a mechanism to operate. In addition, the closer proximity of the CSDs and the S1 domain in RNase II prevents the double-stranded region from even approaching the channel.

This model, together with the supporting data presented here, suggest a mechanism for the degradation of structured RNAs by RNase R. Moreover, they suggest an explanation for RNase R having the ability to degrade through double-stranded RNA, while the closely related protein RNase II stalls as it approaches a duplex. We anticipate that future studies will further clarify the differences between these two related enzymes, and lead to an even more detailed description of RNase R catalysis.

## Materials and Methods

### Materials

Mutagenic primers were synthesized and purified by Sigma Genosys. KOD Hot Start DNA Polymerase was from Novagen. DpnI and bacteriophage T4 polynucleotide kinase were purchased from New England Biolabs, Inc. pETRN<sup>B</sup><sup>15</sup> and purified RNase II<sup>15</sup> were obtained from Dr. A. Malhotra (University of Miami, Miami, FL). Protein assay dye reagent concentrate for Bradford assays was obtained from Bio-Rad Laboratories. Bovine serum albumin was purchased from EM Science. RNA oligonucleotide substrates were synthesized and purified by Dharmacon Inc. [ $\gamma$ -<sup>32</sup>P]ATP was from PerkinElmer Life and Analytical Sciences. SequaGel solutions for preparation of denaturing urea/polyacrylamide gels were purchased from National Diagnostics. Nitrocellulose and Biotyne Plus nylon membranes were from Pall Corp. All other chemicals were reagent grade.

### Cloning of RNase R mutant constructs

pET44R(273-279), pET44R(428-433), pET44R(H456N), pET44R(H565T), and pET44R(R572K) were constructed

by standard site-directed mutagenesis of pET44R using the corresponding primer pairs given in Table 4.<sup>11</sup> The primers required to create pET44R(523/545), pET44R(H565T R572K) and pET44R(620-627) were generated by annealing and extending the respective oligodeoxyribonucleotide pairs given in Table 4. The extended primers were then used to mutate pET44R,<sup>11</sup> using standard site-directed mutagenesis protocols. pET44R(H456N H565T R572K) was constructed through site-directed mutagenesis of pET44R(H565T R572K) using the H456N primers (Table 4).

#### Over-expression of RNase R mutants for preparation of cell extracts

BL21II<sup>-</sup>(DE3)pLysS harboring pET44R,<sup>11</sup> pETRNb,<sup>15</sup> pET44R(273-279), pET44R(428-433), pET44R(H456N), pET44R(523/545), pET44R(H565T), pET44R(R572K), pET44R(620-627), pET44R(H565T R572K) or pET44R(H456N H565T R572K), were grown at 37 °C with shaking to an  $A_{600} \approx 0.6$  in 50 ml of yeast-Tryptone medium supplemented with 100 µg/ml ampicillin, 34 µg/ml chloramphenicol, 25 µg/ml kanamycin and 10 µg/ml tetracycline. Expression was induced by the addition of IPTG to a final concentration of 1 mM. Cells were grown for a further 2 h at 37 °C. After induction, cells from 5 ml of the culture medium were harvested by centrifugation at 5000g for 10 min at 4 °C. The resulting cell pellet was stored frozen at -20 °C. Control uninduced extracts were prepared by growing BL21II<sup>-</sup>(DE3)pLysS harboring pET44R<sup>11</sup> as described above, except that no IPTG was added.

#### Over-expression of RNase R mutants for purification

Wild-type RNase R, RNase R R572K and RNase R H456N H565T R572K were over-expressed from BL21II<sup>-</sup>(DE3)pLysS harboring pET44R,<sup>11</sup> pET44R(R572K) or pET44R(H456N H565T R572K) were grown as described above for the preparation of cell extracts, except that they were grown in 500 ml of yeast-Tryptone medium supplemented with 100 µg/ml ampicillin, 34 µg/ml chloramphenicol, 25 µg/ml kanamycin and 10 µg/ml tetracycline, and the resulting cell pellet was stored frozen at -80 °C.

#### Preparation of cell extracts

Cell pellets prepared as described above were thawed on ice and resuspended in 1.5 ml of 50 mM Tris-HCl (pH 8.0), 300 mM KCl, 0.5 mM EDTA, 5 mM DTT. Cells were lysed by sonication using two 20 s pulses. The lysate was centrifuged at 16,000g for 10 min at 4 °C and the resulting supernatant was retained as the cell extract. The protein concentration of the cell extracts was determined by the Bradford assay,<sup>31</sup> using bovine serum albumin as the standard.

#### Purification of RNase R mutants

Wild-type RNase R, RNase R R572K and RNase R H456N H565T R572K were purified as described for wild-type RNase R.<sup>11</sup>

#### Substrate preparation

The oligoribonucleotide substrates, supplied with the 2'-hydroxyl group protected by an acid-labile O-orthoester group to prevent degradation, were deprotected according to the manufacturer's instructions. The single-stranded oligoribonucleotide substrates used were A<sub>17</sub>, C<sub>17</sub>, U<sub>17</sub>, ss17 (5' CCCCACCACCAUCACUU 3') and ss17-A<sub>17</sub>. These were 5'-labeled with <sup>32</sup>P using T4 polynucleotide kinase and [ $\gamma$ -<sup>32</sup>P]ATP. The ds17-A<sub>17</sub> substrate was prepared by heating a mixture containing 5'-labeled ss17-A<sub>17</sub> and the non-radioactive complementary oligoribonucleotide (5' AAGUGAUGGUGGUGGGG 3') in a 1:1.2 molar ratio, 10 mM Tris-HCl (pH 8.0) and 20 mM KCl in a boiling water-bath and then allowing it to cool slowly to room temperature.

#### Activity assays

RNase R assays were done as described.<sup>16</sup> Briefly, 30 µl reaction mixtures containing 50 mM Tris-HCl (pH 8.0), 300 mM KCl, 0.25 mM MgCl<sub>2</sub>, 5 mM DTT and the amount of substrate and cell extract or purified enzyme as indicated in the figure legends, or for calculation of the rates, 10 µM substrate and an amount of enzyme to ensure that less than 25% of the substrate was degraded. Reactions

**Table 4.** Site-directed mutagenesis primers

Mutant primer	Primer sequence
(273-279)	F: 5' cgc gat tta cgc ctg gtc acc att gat <b>agt gcc agc aca gaa</b> gat atg gac gat gca gtt tac tgc gag aaa aaa cgc 3' R: 5' ggc ttt ttt ctc gca gta aac tgc atc gtc <b>cat atc ttc tgt gct ggc act</b> atc aat ggt gac cag cgg taa atc ggc 3'
(428-433)	F: 5' c cgt gaa gaa cgc ggt ggg atc <b>ttt aaa gat cgc cgg gat</b> cgc aag ttc att ttc aac gct gaa cgc cg 3' R: 5' cg gcg ttc agc gtt gaa aat gaa ctt cgc <b>atc cgg cgc atc ttt aaa</b> gat ccc acc gcg ttc ttc acg g 3'
H456N	F: 5' gaa cag acc cag cgt aac gac gcg <b>aac</b> aaa tta att gaa gag tgc atg att ctg gcg aat atc tgc gc 3' R: 5' gc cga gat att cgc cag aat cat gca ctc ttc aat taa ttt <b>ggt</b> cgc gtc gtt acg ctg ggt ctg ttc 3'
(523/545)	F: 5' g cgt gac tac cgc gag ctg <b>cgc</b> gag tgc gtt gcc gat cgt cct gat gca gaa atg 3' R: 5' cc acg gtt ttc ttg atc gta aat cgc <b>aaa gct ctg</b> cga cgc <b>cgc</b> cag cat ggt <b>atc</b> cag cat ttc tgc atc agg acg atc g 3'
H565T	F: 5' gc ctg gca ttg cag tcc tat gcg <b>acc</b> ttt act tgc cgc att cgt cgt tal cca gac 3' R: 5' gtc tgg ata acg acg aat cgg cga agt aaa <b>ggt</b> cgc ata gga ctg caa tgc cag gc 3'
R572K	F: 5' ggc cac ttt act tgc cgc att cgt <b>aaa</b> tat cca gac ctg acg ctg cac cgc 3' R: 5' gcg gtg cag cgt cag gtc tgg ata <b>ttt</b> acg aat cgg cga agt aaa gtg cgc 3'
H565T R572K	F: 5' gc ctg gca ttg cag tcc tat gcg <b>acc</b> ttt act tgc cgc att cgt 3' R: 3' cg gtg cag cgt cag gtc tgg ata <b>ttt</b> acg aat cgg cga agt aaa <b>ggt</b> cg 3'
(620-627)	F: 5' ggt cag cac tgt tgc atg gcg <b>cgc cgt ctc aac cgc atg gca g</b> 3' R: 3' ctt cag cca gtc agc cac atc gcg <b>ttc tgc cat cgc gtt gag acg g</b> 3'

Nucleotides corresponding to the mutations are in bold. Complementary nucleotides between the forward and reverse primers are in italics. F, forward primer; R, reverse primer.

were incubated at 37 °C and samples were taken at the indicated times, or at regular intervals for determination of the rates, and analyzed by denaturing PAGE (7.5 M urea/20% (w/v) polyacrylamide gel).

### Binding assays

The binding assays, based on the double-filter nucleic acid-binding assay developed by Wong and Lohman,<sup>32</sup> were done as described.<sup>16</sup> Briefly, 20 µl reaction mixtures containing 50 mM Tris-HCl (pH 8.0), 100 mM KCl, 5 mM DTT, 10 mM EDTA, 10% (v/v) glycerol, 200 pM <sup>32</sup>P-labeled substrate and various amounts of purified enzyme were incubated on ice for 30 min. The reaction was applied to a nitrocellulose membrane placed above a nylon membrane in a 96-well dot-blot apparatus (Bio-Rad Laboratories). The fraction of RNA bound at each protein concentration was determined as:

$$\frac{\text{signal}_{\text{nitrocellulose}}}{\text{signal}_{\text{nitrocellulose}} + \text{signal}_{\text{nylon}}}$$

$K_d$  was determined by non-linear regression analysis using a one-site binding hyperbola in Prism (GraphPad Software, Inc).

### Single-turnover experiments

Reactions were done at 15 °C essentially as described.<sup>20</sup> They were initiated by mixing 15 µl of 200 nM RNase R in 50 mM Tris-HCl, 300 mM KCl, 0.25 mM MgCl<sub>2</sub> and 5 mM DTT with 15 µl of 40 nM (5'-<sup>32</sup>P)-labeled ss17-A<sub>17</sub> substrate, also in 50 mM Tris-HCl, 300 mM KCl, 0.25 mM MgCl<sub>2</sub> and 5 mM DTT, using an RQF-3 chemical-quench flow apparatus (KinTek Corporation). The reaction was quenched by the addition of 0.5 M EDTA at time-points ranging from 2 ms to 20 s. The reaction products were analyzed by denaturing PAGE.

### Acknowledgements

This work was supported by grant GM16317 from the National Institutes of Health.

We thank Dr. A. Malhotra, Dr. Y. Zuo and Y. Wang for purified RNase II. We thank Dr. T. K. Harris for the use of his FPLC and chemical-quench flow apparatus. We thank Dr. A. Malhotra, Dr. Y. Zuo and Dr. T. K. Harris for helpful discussions and comments.

### References

- Donovan, W. P. & Kushner, S. R. (1986). Polynucleotide phosphorylase and ribonuclease II are required for cell viability and mRNA turnover in *Escherichia coli* K-12. *Proc. Natl Acad. Sci. USA*, **83**, 120–124.
- Khemici, V. & Carpousis, A. J. (2004). The RNA degradosome and poly(A) polymerase of *Escherichia coli* are required in vivo for the degradation of small mRNA decay intermediates containing REP-stabilizers. *Mol. Microbiol.* **51**, 777–790.
- Cheng, Z. F. & Deutscher, M. P. (2005). An important role for RNase R in mRNA decay. *Mol. Cell*, **17**, 313–318.
- Cheng, Z. F. & Deutscher, M. P. (2003). Quality control of ribosomal RNA mediated by polynucleotide phosphorylase and RNase R. *Proc. Natl Acad. Sci. USA*, **100**, 6388–6393.
- Li, Z., Reimers, S., Pandit, S. & Deutscher, M. P. (2002). RNA quality control: degradation of defective transfer RNA. *EMBO J.* **21**, 1132–1138.
- Mian, I. S. (1997). Comparative sequence analysis of ribonucleases HIII, III, II PH and D. *Nucleic Acids Res.* **25**, 3187–3195.
- Zuo, Y. & Deutscher, M. P. (2001). Exoribonuclease superfamilies: structural analysis and phylogenetic distribution. *Nucleic Acids Res.* **29**, 1017–1026.
- Amblar, M., Barbas, A., Fialho, A. M. & Arraiano, C. M. (2006). Characterization of the functional domains of *Escherichia coli* RNase II. *J. Mol. Biol.* **360**, 921–933.
- Coburn, G. A. & Mackie, G. A. (1996). Overexpression, purification, and properties of *Escherichia coli* ribonuclease II. *J. Biol. Chem.* **271**, 1048–1053.
- Spickler, C. & Mackie, G. A. (2000). Action of RNase II and polynucleotide phosphorylase against RNAs containing stem-loops of defined structure. *J. Bacteriol.* **182**, 2422–2427.
- Vincent, H. A. & Deutscher, M. P. (2006). Substrate recognition and catalysis by the exoribonuclease RNase R. *J. Biol. Chem.* **281**, 29769–29775.
- Cheng, Z. F. & Deutscher, M. P. (2002). Purification and characterization of the *Escherichia coli* exoribonuclease RNase R. Comparison with RNase II. *J. Biol. Chem.* **277**, 21624–21629.
- Cannistraro, V. J. & Kennell, D. (1994). The processive reaction mechanism of ribonuclease II. *J. Mol. Biol.* **243**, 930–943.
- Frazão, C., McVey, C. E., Amblar, M., Barbas, A., Vonrhein, C., Arraiano, C. M. & Carrondo, M. A. (2006). Unravelling the dynamics of RNA degradation by ribonuclease II and its RNA-bound complex. *Nature*, **443**, 110–114.
- Zuo, Y., Vincent, H. A., Zhang, J., Wang, Y., Deutscher, M. P. & Malhotra, A. (2006). Structural basis for processivity and single-strand specificity of RNase II. *Mol. Cell*, **24**, 149–156.
- Vincent, H. A. & Deutscher, M. P. (2008). The roles of individual domains of RNase R in substrate binding and exoribonuclease activity: The nuclease domain is sufficient for digestion of structured RNA. *J. Biol. Chem.* **284**, 486–494.
- Lorentzen, E., Basquin, J., Tomecki, R., Dziembowski, A. & Conti, E. (2008). Structure of the active subunit of the yeast exosome core, Rrp44: diverse modes of substrate recruitment in the RNase II nuclease family. *Mol. Cell*, **29**, 717–728.
- Larkin, M. A., Blackshields, G., Brown, N. P., Chenna, R., McGettigan, P. A., McWilliam, H. *et al.* (2007). Clustal W and Clustal X version 2.0. *Bioinformatics*, **23**, 2947–2948.
- Barbas, A., Matos, R. G., Amblar, M., López-Viñas, E., Gomez-Puertas, P. & Arraiano, C. M. (2008). New insights into the mechanism of RNA degradation by ribonuclease II: identification of the residue responsible for setting the RNase II end product. *J. Biol. Chem.* **283**, 13070–13076.
- Johnson, K. A. (1995). Rapid quench kinetic analysis of polymerases, adenosinetriphosphatases, and enzyme intermediates. *Methods Enzymol.* **249**, 38–61.
- Singer, M. F. & Tolbert, G. (1965). Purification and properties of a potassium-activated phosphodiesterase (RNAase II) from *Escherichia coli*. *Biochemistry*, **4**, 1319–1330.

22. Liu, Q., Greimann, J. C. & Lima, C. D. (2006). Reconstitution, activities, and structure of the eukaryotic RNA exosome. *Cell*, **127**, 1223–1237.
23. Lebreton, A., Tomecki, R., Dziembowski, A. & Seraphin, B. (2008). Endonucleolytic RNA cleavage by a eukaryotic exosome. *Nature*, **456**, 993–996.
24. Schaeffer, D., Tsanova, B., Barbas, A., Reis, F. P., Dastidar, E. G., Sanchez-Rotunno, M. *et al.* (2009). The exosome contains domains with specific endoribonuclease, exoribonuclease and cytoplasmic mRNA decay activities. *Nat. Struct. Mol. Biol.* **16**, 56–62.
25. Schneider, C., Leung, E., Brown, J. & Tollervey, D. (2009). The N-terminal PIN domain of the exosome subunit Rrp44 harbors endonuclease activity and tethers Rrp44 to the yeast core exosome. *Nucleic Acids Res.* In the press. doi:10.1093/nar/gkn1020.
26. Phadtare, S., Inouye, M. & Severinov, K. (2002). The nucleic acid melting activity of Escherichia coli CspE is critical for transcription antitermination and cold acclimation of cells. *J. Biol. Chem.* **277**, 7239–7245.
27. Phadtare, S., Inouye, M. & Severinov, K. (2004). The mechanism of nucleic acid melting by a CspA family protein. *J. Mol. Biol.* **337**, 147–155.
28. Phadtare, S., Tyagi, S., Inouye, M. & Severinov, K. (2002). Three amino acids in Escherichia coli CspE surface-exposed aromatic patch are critical for nucleic acid melting activity leading to transcription antitermination and cold acclimation of cells. *J. Biol. Chem.* **277**, 46706–46711.
29. Singleton, M. R., Dillingham, M. S., Gaudier, M., Kowalczykowski, S. C. & Wigley, D. B. (2004). Crystal structure of RecBCD enzyme reveals a machine for processing DNA breaks. *Nature*, **432**, 187–193.
30. Lohman, T. M. & Ferrari, M. E. (1994). Escherichia coli single-stranded DNA-binding protein: multiple DNA-binding modes and cooperativities. *Annu. Rev. Biochem.* **63**, 527–570.
31. Bradford, M. M. (1976). A rapid and sensitive method for the quantitation of microgram quantities of protein utilizing the principle of protein-dye binding. *Anal. Biochem.* **72**, 248–254.
32. Wong, I. & Lohman, T. M. (1993). A double-filter method for nitrocellulose-filter binding: application to protein-nucleic acid interactions. *Proc. Natl Acad. Sci. USA*, **90**, 5428–5432.